Journal of Computational and Applied Mathematics 337 (2018) 135–149

Contents lists available at ScienceDirect

Journal of Computational and Applied Mathematics

journal homepage: www.elsevier.com/locate/cam

Heterogeneous domain decomposition method for high contrast dense composites

Yuliya Gorb *, Daria Kurzanova

Department of Mathematics, University of Houston, Houston, TX 77204, United States

ARTICLE INFO

Article history:
Received 3 July 2017
Received in revised form 9 January 2018

Keywords:
High contrast
Dense composites
Dirichlet to Neumann map
Heterogeneous domain decomposition method

ABSTRACT

This paper is on numerical treatment of problems that describe high contrast composite materials with complex geometry. In particular, a heterogeneous domain decomposition method for a class of diffusion problems with rapidly oscillating coefficients that also have large variation of values within the domain is proposed. The method combines a FEM discretization in one subdomain with an asymptotic representation of the Dirichlet to Neumann map for the other subdomain. Numerical results that demonstrate the feasibility of the proposed approach are also provided.

1. Introduction

High contrast problems that are characterized by the large or even infinite ratio of the largest and smallest values of coefficients in the corresponding PDE are commonly found in many applications such as porous media flow, composite materials, and electrical impedance tomography. Because of that, the development of efficient numerical schemes for high contrast heterogeneous media has been an active area of research in the past couple of decades, specifically in the design of multiscale solvers.

It was observed that convergence of iterative solvers for the linear systems associated with the high contrast PDEs deteriorates as the contrast in problem coefficients becomes large. Such a loss of efficiency is due to existence of very low eigenvalues in the spectrum of the matrix of the discretized system. Several methods have been proposed to obtain robust and efficient iterative solvers for elliptic problems with highly discontinuous coefficients, see e.g. [1–5] and references therein. Many iterative solvers for elliptic problems with highly heterogeneous coefficients in the *domains of relatively simple geometries* developed by now demonstrate good convergence properties. In this paper, we focus on the problem with high contrast coefficients posed on the domain with *complex geometry*. In particular, we study the case of highly, or even infinitely, conducting heterogeneities irregularly distributed in a domain of finite conductivity and located at distances that are much smaller than their sizes between one another. This leads to significant challenges in numerical methods due to small mesh size needed in the gaps between particles.

To handle this, we employ a *domain decomposition method* (DDM) in this paper. Overall, domain decomposition can be considered as a preconditioner for the iterative solution, but it could also serve as a framework for hybridization of different types of solvers designed for different subdomains. This latter feature is explored in the paper, and a *heterogeneous domain decomposition method* (HDDM), first introduced in [6] (see also [7]), is a domain decomposition method that serves that purpose. Namely, there are two primary reasons to employ an HDDM. The first one is when the underlying problem is of multi-physics nature, and distinct models are used to account for distinct physical processes in subdomains. The other reason

* Corresponding author.
E-mail addresses: gorb@math.uh.edu (Y. Gorb), dariak@math.uh.edu (D. Kurzanova).

https://doi.org/10.1016/j.cam.2018.01.008
0377-0427/

is when one wants to combine different types of approximations in the subdomains. The latter strategy is, in particular, useful when there is a cheaper model in parts of the computational domain where the full model is not needed, and is quite common in the design of *multiscale* FEMs, see e.g. [8].

In this paper, we propose an HDDM for a heterogeneous material that contains a cluster of a large number of densely packed infinitely conducting particles. *Densely packed* (or *closely spaced*, or *closely packed*) particles mean that they are almost touching, and *infinitely* (or *ideally*, or *perfectly*) *conducting* means that their conductivity is infinity with the corresponding potential/temperature on them being constant. We split our domain into nonoverlapping subdomains: a homogeneous one and the other one that contains particles. Normally, a DDM is reduced to a linear system corresponding to the relation enforcing the transmission boundary condition on the interface, called the *Schur complement system*. We observe that one computationally expensive part of the Schur complement that corresponds to the subdomain with particles is the Dirichlet-to-Neumann (DtN) map defined for this subdomain. In Appendix A.1 we define the DtN map and discuss its properties. Also, the DtN map of an infinite contrast medium with particles close to touching was studied in [9]. It is shown that this DtN map can be approximated by a discrete, matrix-valued DtN map that accounts for all the features of the corresponding continuum system, and the asymptotic representation for DtN map was introduced in [9]. We adopt this discrete DtN map in our DDM in the subdomain with particles instead of the direct evaluation of the matrix in the Schur complement system, while we employ a standard finite-element discretization in the other subdomain. Proceeding this way, we actually utilize both features of the HDDM mentioned above, namely, (1) our computational domain is split into two subdomains where distinct physical processes occur, and (2) a computationally inexpensive procedure based on asymptotics developed in [9] is applied in one of those subdomains. Such a hybrid approach yields an accurate approximation of the solution on the interface between the two subdomains, which is demonstrated by our numerical experiments.

The rest of this paper is organized as follows. In Section 2, the mathematical formulation of the problem is presented, the numerical algorithm is described, and challenges of the high contrast dense packing case are highlighted. Section 3 discusses the results on discrete approximation of the DtN map by a matrix-valued one. Numerical experiments of the proposed scheme are given in Section 4. Conclusions are discussed in Section 5. Appendix includes the introduction to the DtN map and provides some auxiliary facts.

2. Problem formulation and domain decomposition method

2.1. Infinite contrast problem formulation

Consider a bounded domain $\hat{\Omega} \subset \mathbb{R}^2$ with piecewise smooth boundary $\partial\hat{\Omega}$ that contains $N \geq 1$ subdomains $\mathcal{D}_i$, which are located at distances much smaller than their sizes from one another. For simplicity, we assume that each $\mathcal{D}_i$ is a disk of radius $R > 0$. Then the distance between two neighboring inclusions $\mathcal{D}_i$ and $\mathcal{D}_j$ is

$$\delta_{ij} = \operatorname{dist}\left\{\mathcal{D}_i, \mathcal{D}_j\right\} \ll R,$$

and denote the typical distance between particles by $\delta \ll R$ that would be rigorously defined below. The union of $\mathcal{D}_i$ is denoted by $\mathcal{D}$. The domain $\hat{\Omega}$ is occupied by the composite medium of uniform conductivity 1 with infinitely conducting particles $\mathcal{D}_i$, $i \in \{1, \ldots, N\}$, where we consider the following problem:

$$\begin{cases} -\triangle u = 0, & x \in \hat{\Omega} \setminus \overline{\mathcal{D}} \\ u = \text{const}, & x \in \partial\mathcal{D}_i,\ i \in \{1, \ldots, N\} \\ \displaystyle\int_{\partial\mathcal{D}_i} \nabla u \cdot \mathbf{n}_i \, ds = 0, & i \in \{1, \ldots, N\} \\ u = g, & x \in \partial\hat{\Omega} \end{cases} \tag{1}$$

where $\mathbf{n}_i$ is the outer unit normal to the surface $\partial\mathcal{D}_i$, and $g \in H^{1/2}(\partial\hat{\Omega})$ is some given function. If

$$u \in V := \left\{u \in H^1(\hat{\Omega} \setminus \overline{\mathcal{D}}) :\ u|_{\partial\mathcal{D}_i} = \text{const},\ i \in \{1, \ldots, N\},\ u|_{\partial\hat{\Omega}} = g\right\}$$

is an electric potential then it attains constant values on the inclusion $\mathcal{D}_i$, $i \in \{1, \ldots, N\}$. These constants are not known a priori and are unknowns of the problem (1) together with $u \in V$. Problem (1) describes the case of perfectly conducting inclusions. With slight abuse of terminology, we refer to problem (1) as the *high contrast* one as it is commonly used in literature.

We assume that all particles $\mathcal{D}_i$ cluster together and locate from the external boundary $\partial\hat{\Omega}$ at distances that are much larger than their sizes R. Then consider a smooth closed curve Γ fully contained in $\hat{\Omega}$ whose interior region include $\overline{\mathcal{D}}$ and such that it splits $\hat{\Omega}$ into two subdomains Ω and Ω', that is, $\hat{\Omega} = \Omega \cup \Gamma \cup \Omega'$. Also, assume that Γ is chosen so that the shortest distance between it and a particle $\mathcal{D}_i$ is of order δ, hence,

$$\delta_i = \operatorname{dist}\{\mathcal{D}_i, \Gamma\} = O(\delta) \ll R.$$

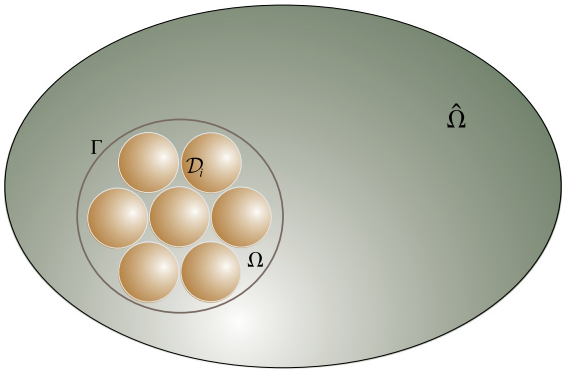

Fig. 1. The domain $\hat{\Omega}$ with highly conducting inclusions $\mathcal{D}_i$, $i \in \{1, \dots, N\}$, that are concentrated in the subregion $\Omega \subset\subset \hat{\Omega}$.

Without loss of generality, assume also that the domain Ω is a disk of radius $L \gg R$, thus, $\Omega \subset\subset \hat{\Omega}$ and $\Gamma = \partial\Omega$, see Fig. 1. With that, the subdomain $\Omega' = \hat{\Omega} \setminus \overline{\Omega}$ is occupied by the homogeneous conducting material of constant conductivity equal to 1. We remark that the choice for such a split of $\hat{\Omega}$ is motivated by the fact that a FEM discretization in the subdomain Ω' is cheap while it is not so in Ω. Because of this, we propose to design a *heterogeneous domain decomposition* introduced in [6,7] to bridge the domain decomposition methodology with mathematical modeling. Indeed, our domain partition now involves different models in different subdomains, and the asymptotic approximation for the energy in subdomain Ω that is readily available thanks to the study [9] together with FEM discretization in the subdomain Ω' leads to a significant reduction of computation complexity.

Before we introduce our HDDM methodology, in the next sections, we describe the classical DDM for (1) in $\hat{\Omega} = \Omega \cup \Gamma \cup \Omega'$ and comment how the DtN map, or rather its approximation, can be applied.

2.2. Classical DDM for Ω, Ω' and Γ

2.2.1. Discretization of continuous problem

Consider a confirming quasi-uniform triangulation $\hat{\Omega}_h$ of domain $\hat{\Omega}$ with the corresponding triangulations Ω_h, Ω'_h of the domains Ω, Ω', respectively. We require that the nodes of triangulation $\hat{\Omega}_h$ match the interface Γ and the external boundary $\partial\hat{\Omega}$. Then the classical FEM discretization of (1) on this $\hat{\Omega}_h$ using piecewise linear finite elements results in a linear system

$$\boldsymbol{\mathcal{A}}\,\overline{u} = \overline{F}, \tag{2}$$

with a symmetric and positive definite matrix $\boldsymbol{\mathcal{A}}$. From now on, the *bar*-quantities will indicate vectors in the corresponding finite-dimensional space. The degrees of freedom of (2) are split into the degrees belonging to Ω, indicated by the subscript 1, those internal to Ω', indicated by the subscript 2, those belonging to the interface Γ, indicated by the subscript Γ, and those belonging to the external boundary $\partial\hat{\Omega}$, indicated by the subscript D. With that, the components of the linear system (2) are as follows:

$$\begin{pmatrix} A_{11} & A_{1\Gamma} & 0 \\ A_{1\Gamma}^T & A_{\Gamma\Gamma} & A_{2\Gamma} \\ 0 & A_{2\Gamma}^T & A_{22} \end{pmatrix} \begin{pmatrix} \overline{u}_1 \\ \overline{u}_\Gamma \\ \overline{u}_2 \end{pmatrix} = \begin{pmatrix} 0 \\ 0 \\ -A_{2\mathrm{D}}\overline{g}_\mathrm{D} \end{pmatrix}, \tag{3}$$

where the vector $\overline{g}_\mathrm{D}$ is composed of values of function g at the points of discretization on the external boundary $\partial\hat{\Omega}$, and $A_{2\mathrm{D}}$ is a stiffness matrix assembled using nodes in Ω'_h and on $\partial\hat{\Omega}$. Entries of the matrix $\boldsymbol{\mathcal{A}}$ and the vector $\overline{u} = \left(\overline{u}_1\ \overline{u}_\Gamma\ \overline{u}_2\right)^T$ in (2)–(3) correspond to the interior nodes of $\hat{\Omega}_h$ only, while the right-hand side vector $\overline{F} = \left(0\,0\ -A_{2\mathrm{D}}\overline{g}_\mathrm{D}\right)^T$ captures the contribution of nodes on $\partial\hat{\Omega}$.

The stiffness matrix $A_{\Gamma\Gamma}$ on the interface Γ is also obtained by assembling the corresponding components contributed by the subdomains Ω_h and Ω'_h and can be written as $A_{\Gamma\Gamma} = A^{(1)}_{\Gamma\Gamma} + A^{(2)}_{\Gamma\Gamma}$. With that, below we will distinguish the following blocks of the stiffness matrix $\boldsymbol{\mathcal{A}}$:

$$\begin{pmatrix} A_{11} & A_{1\Gamma} \\ A_{1\Gamma}^T & A^{(1)}_{\Gamma\Gamma} \end{pmatrix}, \quad \text{and} \quad \begin{pmatrix} A^{(2)}_{\Gamma\Gamma} & A_{2\Gamma} \\ A_{2\Gamma}^T & A_{22} \end{pmatrix},$$

corresponding to the two subdomains Ω_h and Ω'_h, respectively.

2.2.2. Schur complement system

The usual first step of many iterative domain decomposition methods is the elimination of interior unknowns $\overline{u}_1$ and $\overline{u}_2$, which reduces the system (3) to the *Schur complement system* for $\overline{u}_\Gamma$:

$$\mathrm{S}\overline{u}_\Gamma = \overline{g}^{(2)}_\Gamma, \quad \text{where} \quad \mathrm{S} = \mathrm{S}^{(1)} + \mathrm{S}^{(2)}, \tag{4}$$

with

$$\mathrm{S}^{(1)} = A^{(1)}_{\Gamma\Gamma} - A^T_{1\Gamma}A^{-1}_{11}A_{1\Gamma}, \quad \mathrm{S}^{(2)} = A^{(2)}_{\Gamma\Gamma} - A_{2\Gamma}A^{-1}_{22}A^T_{2\Gamma}, \quad \overline{g}^{(2)}_\Gamma = A_{2\Gamma}A^{-1}_{22}A_{2\mathrm{D}}\overline{g}_\mathrm{D}, \tag{5}$$

see [10] for the detailed discussion of the construction. Matrix S is usually referred to as *Schur complement* to the unknowns on Γ. Our matrix slightly differs from the classic case as in our notation subscript 2 does *not* include nodes on the external boundary indicated by the subscript D. Observe, that once system (4) is solved, the internal components could be found from

$$\overline{u}_1 = -A^{-1}_{11}A_{1\Gamma}\overline{u}_\Gamma, \quad \overline{u}_2 = -A^{-1}_{22}A_{2\mathrm{D}}\overline{g}_\mathrm{D} - A^{-1}_{22}A_{2\Gamma}\overline{u}_\Gamma. \tag{6}$$

Next, we derive one more auxiliary approximation that we utilize later in our method. Consider the discrete analog of the Neumann problem in Ω, see [11],

$$\begin{pmatrix} A_{11} & A_{1\Gamma} \\ A^T_{1\Gamma} & A^{(1)}_{\Gamma\Gamma} \end{pmatrix} \begin{pmatrix} \overline{u}_1 \\ \overline{u}_\Gamma \end{pmatrix} = \begin{pmatrix} 0 \\ \overline{\lambda}_{1\Gamma} \end{pmatrix},$$

where $\overline{\lambda}_{1\Gamma}$ is an approximation for the weak normal derivative of u_1 on the interface Γ, that is,

$$\overline{\lambda}_{1\Gamma} = A^T_{1\Gamma}\overline{u}_1 + A^{(1)}_{\Gamma\Gamma}\overline{u}_\Gamma = \mathrm{S}^{(1)}\overline{u}_\Gamma, \tag{7}$$

where we applied the definition of $\mathrm{S}^{(1)}$ as in (5).

2.2.3. The Dirichlet–Neumann algorithm

In this paper, we utilize the Dirichlet–Neumann domain decomposition method, see e.g. [10] and apply it to the case when Ω is embedded in $\hat{\Omega}$. In this algorithm, each iteration step consists of two fractional steps: Dirichlet problem in subdomain Ω and mixed Neumann–Dirichlet problem in subdomain Ω' with the Neumann condition on the interface Γ as determined by the solution in Ω of the previous step and the Dirichlet data on $\partial\hat{\Omega}$. The next iteration is chosen as a linear combination of the trace of the solution in Ω' and the solution on the interface Γ obtained in the previous iteration with a suitably chosen relaxation parameter $\vartheta \in (0, \vartheta_{max})$ to ensure convergence of the method. In terms of differential operators the algorithm described above is as follows:

1. Choose an initial guess: $u^0_\Gamma \in H^{1/2}(\Gamma)$.
2. For any $n \in \mathbb{N}$, until convergence, find $u^{n+1/2}_1 \in H^1(\Omega)$ that solves

$$(\mathsf{D}): \quad \begin{cases} -\triangle u^{n+1/2}_1 = 0 & \text{in } \Omega, \\ u^{n+1/2}_1 = u^n_\Gamma & \text{on } \Gamma, \end{cases} \tag{8}$$

   where (D) indicates the problem with the Dirichlet boundary conditions on Γ.
3. Evaluate the weak normal derivative $\lambda^{n+1/2}_{1\Gamma} = \nabla u^{n+1/2}_1 \cdot \mathbf{n}_1$ on Γ, where $\mathbf{n}_1$ is the unit outward normal to $\partial\Omega = \Gamma$.
4. Find the function $u^{n+1}_2 \in H^1(\Omega')$ by solving

$$(\mathsf{D}+\mathsf{N}): \quad \begin{cases} -\triangle u^{n+1}_2 = 0 & \text{in } \Omega', \\ \nabla u^{n+1}_2 \cdot \mathbf{n}_2 = -\lambda^{n+1/2}_{1\Gamma} & \text{on } \Gamma, \\ u^{n+1}_2 = g & \text{on } \partial\hat{\Omega}, \end{cases} \tag{9}$$

   where (D + N) indicates the problem with Neumann boundary conditions on Γ and Dirichlet conditions on $\partial\hat{\Omega}$, and $\mathbf{n}_2 = -\mathbf{n}_1$.
5. Update $u^{n+1}_\Gamma = \vartheta u^{n+1}_2 + (1-\vartheta)u^n_\Gamma$ on Γ for some $\vartheta \in (0, \vartheta_{max})$.
6. Repeat until convergence.

With use of the approximations given above, the corresponding iteration for the discrete problem is as follows. Let $M > 0$ be the number of degrees of freedom on the interface Γ. Then:

1. Choose an initial vector $\overline{u}^0_\Gamma \in \mathbb{R}^M$ (below, in our numerical experiments we initialize it with zero vector).
2. For any $n \in \mathbb{N}$, until convergence, find an approximation $\overline{u}^{n+1/2}_1$ of $u^{n+1/2}_1$ that solves the discrete analog of (8):

$$(\mathsf{D}): \quad A_{11}\overline{u}^{n+1/2}_1 + A_{1\Gamma}\overline{u}^n_\Gamma = 0.$$

3. Compute the vector $\overline{\lambda}_{1\Gamma}^{n+1/2} \in \mathbb{R}^M$, which is the discrete analog of the weak normal derivative $\lambda_{1\Gamma}^{n+1/2}$ via

$$\overline{\lambda}_{1\Gamma}^{n+1/2} = A_{1\Gamma}^T \overline{u}_1^{n+1/2} + A_{\Gamma\Gamma}^{(1)} \overline{u}_\Gamma^n. \tag{10}$$

Now eliminate $\overline{u}_1^{n+1/2}$ from (D), hence, $\overline{u}_1^{n+1/2} = -A_{11}^{-1} A_{1\Gamma} \overline{u}_\Gamma^n$ and substitute this in (10) to obtain

$$\overline{\lambda}_{1\Gamma}^{n+1/2} = -A_{1\Gamma}^T A_{11}^{-1} A_{1\Gamma} \overline{u}_\Gamma^n + A_{\Gamma\Gamma}^{(1)} \overline{u}_\Gamma^n = \mathrm{S}^{(1)} \overline{u}_\Gamma^n. \tag{11}$$

4. Find an approximation $\overline{u}_2^{n+1}$ of the function u_2^{n+1} in the domain Ω' that solves the discrete analog of (9):

$$(\mathrm{D}+\mathrm{N}): \quad \begin{pmatrix} A_{\Gamma\Gamma}^{(2)} & A_{2\Gamma} \\ A_{2\Gamma}^T & A_{22} \end{pmatrix} \begin{pmatrix} \overline{u}_{2\Gamma}^{n+1} \\ \overline{u}_2^{n+1} \end{pmatrix} = \begin{pmatrix} -\overline{\lambda}_{1\Gamma}^{n+1/2} \\ -A_{2\mathrm{D}} \overline{g}_\mathrm{D} \end{pmatrix}, \tag{12}$$

where $\overline{u}_{2\Gamma}^{n+1}$ is an approximation of the trace of u_2 of (9). The nonhomogeneous Dirichlet boundary condition on $\partial\hat{\Omega}$ is already accounted by the system (12), similarly to (3), and the problem (12) is formulated for the interior nodes only.
5. Update $\overline{u}_\Gamma^{n+1} = \vartheta \overline{u}_{2\Gamma}^{n+1} + (1-\vartheta)\overline{u}_\Gamma^n$ for some $\vartheta \in (0, \vartheta_{max})$.
6. Finally, eliminating $\overline{u}_2^{n+1}$ in (12) and applying relation (11) yields the following equation:

$$\mathrm{S}^{(2)} \left(\overline{u}_\Gamma^{n+1} - \overline{u}_\Gamma^n \right) = \vartheta \left(\overline{g}_\Gamma^{(2)} - S \overline{u}_\Gamma^n \right). \tag{13}$$

We observe that (13) is a preconditioned Richardson iteration for the Schur complement system (4) with the preconditioner $\mathrm{S}^{(2)}$ and the relaxation parameter ϑ.

2.3. Challenges of the problem with a densely packed subdomain Ω

Typically, nonoverlapping DDM algorithms involve solving a Schur complement system (4) using a suitable interface preconditioner, and (13) illustrates that this preconditioner is $\mathrm{S}^{(2)}$. Since matrix $\mathrm{S}^{(2)}$ is associated with the domain Ω' of uniform conductivity, we assume that $\mathrm{S}^{(2)}$ is feasible to compute. On the other hand, solving for $\mathrm{S}^{(1)}$ that corresponds to the domain Ω that contains closely spaced particles of infinite conductivity by direct methods can be expensive. This is because of complex geometry of fine-scale features in Ω that, in particular, causes a large size of the matrix A_{11} in (3). Therefore, it is desirable to seek for a *cheaper* approximation of $\mathrm{S}^{(1)}$, which we will study in some detail in the rest of the paper. Below, we propose an approximation of $\mathrm{S}^{(1)}$ that could be used to make the algorithm described in Section 2.2.3 applicable in practice. It is based on the observation that the relation (7) between the weak Neumann derivative approximation $\overline{\lambda}_{1\Gamma}$ of u_1 on the interface Γ and the Schur complement $\mathrm{S}^{(1)}$ corresponding to the domain Ω actually defines a FEM approximation of the DtN map Λ^{DtN} associated with the domain Ω. Hence, we suggest to find an approximation $\mathbf{\Lambda}$ of the DtN map Λ^{DtN} that would be cheaper than direct evaluation of $\mathrm{S}^{(1)}$. For this, we propose to utilize a discrete, matrix-valued DtN map $\mathbf{\Lambda}$ as introduced in the next section. It is given by an asymptotic representation derived in [9] in the regime when the typical interparticle distance δ is much smaller than the sizes R of particles and the diameter L of Ω: $\delta \ll R \ll L$. In particular, this approach allows us to bypass computationally expensive numerical evaluation of the solution u_1 in the domain Ω that contains closely spaced perfectly conducting particles. Meanwhile, one can obtain an approximate solution to u_1 in the domain Ω' using a standard FEM discretization. With this, we will derive an approach that combines an asymptotic method defined in the domain Ω with a finite-element one in Ω' within the framework of the domain decomposition methods and leads to a *heterogeneous DDM*, as announced above.

3. Construction of the discrete DtN map $\mathbf{\Lambda}$

3.1. Asymptotic approximation of the DtN map Λ^{DtN}

In this section, we review results obtained in [9]. This paper discusses the continuous DtN map of a diffusion PDE of the type (1) defined in a domain Ω with a piece-wise smooth boundary Γ. A Dirichlet-to-Neumann (DtN) map Λ^{DtN} for this problem takes an arbitrary boundary voltage u on the boundary $\Gamma = \partial\Omega$ to the associated current flux on Γ via (33), where the coefficient $\sigma(\mathbf{x})$ has infinite contrast and varies rapidly within the domain (see detailed discussion on DtN map in Appendix A.1). It is shown in [9] that this Λ^{DtN} can be approximated by the *matrix-valued DtN map* $\mathbf{\Lambda}$ as given in Theorem 1 below.

Recall that the domain Ω is a disk of radius L packed with N perfectly conducting inclusions $\mathcal{D}_i$, which are identical disks of radius $R \ll L$. It is also assumed that a typical distance between inclusions δ is much smaller than their sizes, that is, $\delta \ll R$. The interparticle distance parameter δ is defined through the notion of *neighboring* inclusions, which is as follows. Let $\mathcal{V}_i$ be the Voronoi cell, see e.g. [12], constructed for inclusion $\mathcal{D}_i$, $i \in \{1, \dots, N\}$, via

$$\mathcal{V}_i = \left\{ \mathbf{x} \in \Omega \text{ such that } |\mathbf{x} - \mathbf{x}_i| \le |\mathbf{x} - \mathbf{x}_j|, \text{ for all } j \in \{1, \dots, N\},\ j \ne i \right\}.$$

The inclusions $\mathcal{D}_i$ and $\mathcal{D}_j$ are said to be neighbors if their Voronoi cells $\mathcal{V}_i$ and $\mathcal{V}_j$ share an edge. For each inclusion $\mathcal{D}_i$ denote a set of indices of the neighboring inclusions

$$\mathcal{N}_i = \left\{ j \in \{1, \dots, N\}\,,\ \mathcal{D}_j \ \text{is a neighbor to } \mathcal{D}_i \right\}.$$

Recall that the typical distance between two neighboring inclusions is defined as $\delta_{ij} \ll R$, where $i \in \{1, \dots, N\}$ and $j \in \mathcal{N}_i$. Also, suppose that there are N_Γ inclusions that neighbor the boundary, that is, $\mathcal{V}_i \cap \Gamma \neq \emptyset, i \in \{1, \dots, N_\Gamma\}$. Then define the typical distance between such an inclusion and the boundary Γ as

$$\delta_i = \operatorname{dist}\{\mathcal{D}_i, \Gamma\}\,, \quad \delta_i \ll R.$$

The inclusions are numbered starting with those that are adjacent to the boundary Γ and counted clockwise. Hence, inclusion $\mathcal{D}_i$ neighbors the boundary if $i \in \{1, \dots, N_\Gamma\}$, and $\mathcal{D}_i$ is an interior inclusion if $i \in \{N_\Gamma + 1, \dots, N\}$. Then the interparticle distance parameter δ is defined by

$$\delta = \max\left\{ \{\delta_{ij} :\ i \in \{1, \dots, N\}\,,\ j \in \mathcal{N}_i\}, \{\delta_i :\ i \in \{1, \dots, N_\Gamma\}\} \right\}.$$

Since Γ is a circle, we parametrize it by angle $\theta \in [0, 2\pi)$, and present a boundary potential $\psi \in H^{1/2}_\dagger(\Gamma)$ with $H^{1/2}_\dagger(\Gamma)$ defined in (35), as a truncated Fourier series

$$\psi(\theta) = \sum_{k=1}^{K} [a_k \cos k\theta + b_k \sin k\theta] =: \sum_{k=1}^{K} \psi_k(\theta), \tag{14}$$

for a sufficiently *large* $K \gg 1$, which is chosen depending on the precision of the discretization of ψ on Γ. For the discretization of the boundary Γ, we choose $M \gg 1$ points θ_i in such a way that N_Γ points of this discretization will be the closest to the inclusions $\mathcal{D}_i, i \in \{1, \dots, N_\Gamma\}$ adjacent to Γ than any other points. Denote the set of indices of such points on Γ by $\mathcal{J}_\Gamma \subset \{1, \dots, M\}$ with $|\mathcal{J}_\Gamma| = N_\Gamma$. Note that due to the decomposition chosen in (14), we need to truncate the Fourier series at $K = M/2$. Because of that, we discretize the boundary Γ with an even number M of points θ_i.

The DtN map $\Lambda^{\mathrm{DtN}} : H^{1/2}(\Gamma) \to H^{-1/2}(\Gamma)$ on the interface Γ corresponding to u defined by (1) is given by

$$\langle \psi, \Lambda^{\mathrm{DtN}} \psi \rangle = \int_{\Omega \setminus \mathcal{D}} |\nabla u|^2 \, d\mathbf{x} = \int_\Gamma \psi\ \Lambda^{\mathrm{DtN}} \psi \ ds, \tag{15}$$

with $u|_\Gamma = \psi$ (see Appendix A.1 for the detailed discussion on the DtN map). Then, the asymptotic representation for the DtN map Λ^{DtN} in the regime of scale separation between the small interparticle distance δ, the particles' radius R, and the size L of the domain Ω is given in the following theorem formulated and proven in [9].

Theorem 1. *For a potential ψ of the form (14), the asymptotic representation for Λ^{DtN} is*

$$\langle \psi, \Lambda^{DtN} \psi \rangle = 2 \left[\mathcal{E}^{net}[\overline{\Psi}(\psi)] + \frac{1}{2} \langle \psi, \Lambda_0 \psi \rangle + \mathcal{R}[\psi] \right] [1 + o(1)]\,, \quad \text{for } \delta \ll R \ll L. \tag{16}$$

The first term of (16) is the discrete energy $\mathcal{E}^{net}[\overline{\Psi}(\psi)]$ of the resistor network given by

$$\mathcal{E}^{net}[\overline{\Psi}(\psi)] = \min_{\overline{\mathcal{U}} \in \mathbb{R}^N} \left\{ \sum_{m=1}^{N_\Gamma} \frac{\sigma_m}{2} (\mathcal{U}_m - \Psi_m)^2 + \frac{1}{2} \sum_{m=1}^{N} \sum_{n \in \mathcal{N}_m} \frac{\sigma_{mn}}{2} (\mathcal{U}_m - \mathcal{U}_n)^2 \right\}, \tag{17}$$

with vector $\overline{\Psi}(\psi) = (\Psi_1, \dots, \Psi_{N_\Gamma})^T$ of boundary potentials defined by

$$\Psi_m = \sum_{k=1}^{K} \psi_k(\theta_{\kappa_m}) e^{-\frac{k\sqrt{2R\delta_m}}{L}}, \quad m \in \{1, \dots, N_\Gamma\},\ \kappa_m \in \mathcal{J}_\Gamma, \tag{18}$$

where $\theta_{\kappa_m} \in \Gamma$, $\kappa_m \in \mathcal{J}_\Gamma$, is the point on Γ closest to the inclusion $\mathcal{D}_m$, $m \in \{1, \dots, N_\Gamma\}$, and ψ_k is introduced in (14). The local conductivities σ_{mn} and σ_m in (17) are defined by

$$\sigma_{mn} = \pi \sqrt{\frac{R}{\delta_{mn}}} \ \text{ if } m \in \{1, \dots, N\},\ n \in \mathcal{N}_m, \quad \sigma_m = \pi \sqrt{\frac{2R}{\delta_m}} \ \text{ if } m \in \{1, \dots, N_\Gamma\}, \tag{19}$$

where δ_{mn} is the shortest distance between two neighboring particles $\mathcal{D}_m$ and $\mathcal{D}_n$, and δ_m is the distance between $\mathcal{D}_m$ and boundary Γ.

The second term in (16) is the quadratic form of the DtN map Λ_0 of the reference medium, which is a homogeneous one with uniform conductivity $\sigma = 1$, that is, without inclusions.

The last term $\mathcal{R}[\psi]$ of (16) is given by

$$\begin{aligned} \mathcal{R}[\psi] = \sum_{m=1}^{N_\Gamma} \sum_{i,j=1}^{K} e^{-|i-j|\frac{\sqrt{2R\delta_m}}{L}} \mathcal{R}_{m,i\wedge j} \big\{ & (a_i a_j + b_i b_j) \cos[(i-j)\theta_m] \\ & + (b_i a_j - a_i b_j) \sin[(i-j)\theta_m] \big\}, \end{aligned} \tag{20}$$

where $i \wedge j = \min\{i, j\}$, a_k, b_k are Fourier coefficients of ψ from (14), and $\mathcal{R}_{m,k}$ is defined by

$$\mathcal{R}_{m,k} = \frac{\sigma_m}{4}\left[\sqrt{\frac{2k\delta_m}{\pi L}}Li_{\mathbf{1/2}}\left(e^{-\frac{2k\delta_m}{L}}\right) - e^{-\frac{2k\sqrt{2R\delta_m}}{L}}\right],\ k \in \{1,\dots,K\},\ m \in \{1,\dots,N_\Gamma\}, \tag{21}$$

in terms of the polylogarithm function $Li_{\mathbf{1/2}}$, see e.g. [13], and local conductivity σ_i of (19).

3.2. Construction of the discrete DtN map $\mathbf{\Lambda}$

We rewrite (16) as

$$\langle\psi, \Lambda^{\mathrm{DtN}}\psi\rangle = (\overline{\psi}, \mathbf{\Lambda}\overline{\psi})[1 + o(1)] \quad \text{with} \quad (\overline{\psi}, \mathbf{\Lambda}\overline{\psi}) = 2\mathcal{E}^{\mathrm{net}}[\overline{\Psi}(\psi)] + \langle\psi, \Lambda_0\psi\rangle + 2\mathcal{R}[\psi],$$

where $\overline{\psi} \in \mathbb{R}^M$ is the vector that corresponds to the FEM approximation of $\psi \in H^{1/2}(\Gamma)$, $\mathbf{\Lambda} \in \mathbb{R}^{M\times M}$ is a matrix-valued DtN map approximation, hereafter referred to as a *discrete DtN map*, and $(\cdot,\cdot)$ is the standard dot-product in $\mathbb{R}^M$. In this section we use the result of Theorem 1 to construct $\mathbf{\Lambda}$. We discretize the boundary Γ with points θ_i, $i \in \{1,\dots,M\}$ as announced above. Then the discrete DtN map $\mathbf{\Lambda} \in \mathbb{R}^{M\times M}$ is a symmetric positive semi-definite matrix, whose rank is $M-1$ and the kernel spans the vector $\mathbf{1}_M \in \mathbb{R}^M$ of units. To find the entries Λ_{ij} of $\mathbf{\Lambda}$, we use the approximation to quadratic form (16) and the discrete analog of polarization identity (36) via the system of equations

$$\mathbf{\Psi}^T\mathbf{\Lambda}\mathbf{\Psi} = \mathbf{\Upsilon}, \tag{22}$$

where the columns of the matrix $\mathbf{\Psi} = [\overline{\psi}_1,\dots,\overline{\psi}_{M-1}] \in \mathbb{R}^{M\times(M-1)}$ form a basis in $\mathbb{R}^{M-1}$. These columns of the matrix $\mathbf{\Psi}$ correspond to a set of $M-1$ linearly independent functions $\Xi := \{\psi_1,\dots,\psi_{M-1}\}$ that are chosen as the first $M-1$ functions from the set $\left\{\frac{\cos k\theta}{\sqrt{\pi}},\ \frac{\sin k\theta}{\sqrt{\pi}}\right\}_{k=1}^{\infty}$ of L^2-basis, that is,

$$\Xi = \left\{\frac{\cos\theta}{\sqrt{\pi}},\dots,\frac{\cos\frac{M}{2}\theta}{\sqrt{\pi}},\ \frac{\sin\theta}{\sqrt{\pi}},\dots,\frac{\sin(\frac{M}{2}-1)\theta}{\sqrt{\pi}}\right\}. \tag{23}$$

Then the entries of the matrix $\mathbf{\Psi} = [\Psi_{ij}]$ are given by

$$\Psi_{ij} = \psi_j(\theta_i), \quad i \in \{1,\dots,M\}, \quad j \in \{1,\dots,M-1\}, \quad \theta_i \in \Gamma, \quad \psi_j \in \Xi, \tag{24}$$

hence,

$$\mathbf{\Psi} = \frac{1}{\sqrt{\pi}}\begin{pmatrix} \cos\theta_1 & \dots & \cos\frac{M}{2}\theta_1 & \sin\theta_1 & \dots & \sin(\frac{M}{2}-1)\theta_1 \\ \vdots & \ddots & \vdots & \vdots & \ddots & \ddots \\ \cos\theta_M & \dots & \cos\frac{M}{2}\theta_M & \sin\theta_M & \dots & \sin(\frac{M}{2}-1)\theta_M \end{pmatrix}. \tag{25}$$

Entries of the right hand side $\mathbf{\Upsilon} \in \mathbb{R}^{(M-1)\times(M-1)}$ of (22) are computed by the asymptotic procedure described by Theorem 1 and the discrete polarization identity:

$$\Upsilon_{i,j} = \frac{1}{4}\left\{\left(\overline{\psi}_i + \overline{\psi}_j, \Lambda(\overline{\psi}_i + \overline{\psi}_j)\right) - \left(\overline{\psi}_i - \overline{\psi}_j, \Lambda(\overline{\psi}_i - \overline{\psi}_j)\right)\right\}.$$

More specifically, the matrix $\mathbf{\Upsilon}$ is given by

$$\begin{aligned}\Upsilon_{i,j} = {} & \frac{1}{2}\left\{\mathcal{E}^{\mathrm{net}}[\overline{\Psi}(\psi_i+\psi_j)] + \frac{1}{2}\langle\psi_i+\psi_j, \Lambda_0(\psi_i+\psi_j)\rangle + \mathcal{R}[\psi_i+\psi_j]\right\} \\ & - \frac{1}{2}\left\{\mathcal{E}^{\mathrm{net}}[\overline{\Psi}(\psi_i-\psi_j)] + \frac{1}{2}\langle\psi_i-\psi_j, \Lambda_0(\psi_i-\psi_j)\rangle + \mathcal{R}[\psi_i-\psi_j]\right\}, \quad \psi_i, \psi_j \in \Xi.\end{aligned}$$

We split $\Upsilon_{i,j}$ into a sum of three terms to treat them separately

$$\begin{aligned}\Upsilon^{(1)}_{i,j} &= \frac{1}{2}\left\{\mathcal{E}^{\mathrm{net}}[\overline{\Psi}(\psi_i+\psi_j)] - \mathcal{E}^{\mathrm{net}}[\overline{\Psi}(\psi_i-\psi_j)]\right\}, \quad \psi_i, \psi_j \in \Xi, \\ \Upsilon^{(2)}_{i,j} &= \frac{1}{4}\left\{\left\langle\psi_i+\psi_j, \Lambda_0(\psi_i+\psi_j)\right\rangle - \left\langle\psi_i-\psi_j, \Lambda_0(\psi_i-\psi_j)\right\rangle\right\}, \quad \psi_i, \psi_j \in \Xi, \\ \Upsilon^{(3)}_{i,j} &= \frac{1}{2}\left\{\mathcal{R}[\psi_i+\psi_j] - \mathcal{R}[\psi_i-\psi_j]\right\} \quad \psi_i, \psi_j \in \Xi.\end{aligned} \tag{26}$$

Later, we show how much influence each term $\Upsilon^{(\ell)}_{i,j}$, $\ell \in \{1,2,3\}$, has on $\mathbf{\Lambda}$ depending on k for the boundary function ψ given by a single mode $k \in \{1,\dots,K\}$, see Table 1.

Table 1
Energy terms for $\psi = \cos k\theta$.

k	$\mathcal{E}^{\text{net}}[\mathbf{\Psi}(\psi)]$	$\langle \psi, \Lambda_0 \psi \rangle$	$\mathcal{R}_k[\psi]$
1	17.72	3.14	0.23
10	9.51	31.42	32
50	0.6	157.08	57.39
100	0.02	314.16	44.14
200	$1.88 \cdot 10^{-5}$	628.32	25.42
500	$1.8 \cdot 10^{-14}$	1570.8	5.28

Once matrix $\mathbf{\Upsilon}$ is constructed using (26), we recover the discrete DtN map $\mathbf{\Lambda}$ from (22). A detailed description in the following subsections shows how to compute entries $\Upsilon^{(1)}_{i,j}$, $\Upsilon^{(2)}_{i,j}$ and $\Upsilon^{(3)}_{i,j}$.

3.2.1. Evaluation of entries $\Upsilon^{(1)}_{i,j}$

In order to construct the $\Upsilon^{(1)}_{i,j}$ by (26), which corresponds to the contribution of the resistor network, we need to consider boundary potential vectors $\overline{\Psi}(\psi_i)$, $\overline{\Psi}(\psi_j) \in \mathbb{R}^{N_\Gamma}$. To specify entries of $\overline{\Psi}(\psi_i) = (\Psi^i_1, \dots, \Psi^i_{N_\Gamma})$, we suppose that the boundary potential is given by a single Fourier mode $\psi = \psi_i \in \Xi$, $i \in \{1, \dots, M-1\}$. Let $k_i \in \{1, \dots, K\}$ be the Fourier frequency mode of $\psi_i \in \Xi$, that is,

$$k_i = \begin{cases} i, & \text{if } i \le M/2 \\ i - M/2, & \text{if } i > M/2 \end{cases} \tag{27}$$

and $\theta_{\kappa_m} \in \Gamma$, $\kappa_m \in \mathcal{J}_\Gamma$, be the point of discretization of Γ that is adjacent to the neighboring particle $\mathcal{D}_m$, $m \in \{1, \dots .N_\Gamma\}$. With this, entries of $\overline{\Psi}(\psi_i)$ are given by

$$\Psi^i_m = \psi_i(\theta_{\kappa_m}) e^{-\frac{k_i\sqrt{2R\delta_m}}{L}}, \quad \kappa_m \in \mathcal{J}_\Gamma, \quad m \in \{1, \dots, N_\Gamma\}, \quad i \in \{1, \dots, M-1\},$$

where δ_m is the distance between $\mathcal{D}_m$ and Γ, R is the radius of the particle, and L is the radius of Ω. We also recall that vector $\overline{\Psi}(\psi_i)$ forms the ith column of the matrix $\mathbf{\Psi}$.

With two boundary potential vectors $\overline{\Psi}(\psi_i)$, $\overline{\Psi}(\psi_j) \in \mathbb{R}^{N_\Gamma}$ chosen this way, one can find minimizers $\overline{\mathcal{U}}^i$, $\overline{\mathcal{U}}^j \in \mathbb{R}^N$ of the discrete energy (17), respectively, corresponding to these boundary potentials. Finally, applying the results of lemmas stated and proved in Appendix A.2 for the discrete energy (17), we conclude that

$$\begin{aligned} \Upsilon^{(1)}_{i,j} = \frac{1}{2}\Bigg\{ &\sum_{m=1}^{N_\Gamma} \frac{\sigma_m}{2} \left[(\mathcal{U}^i_m + \mathcal{U}^j_m) - (\Psi^i_m + \Psi^j_m)\right]^2 + \frac{1}{2}\sum_{m=1}^{N}\sum_{n\in\mathcal{N}_m} \frac{\sigma_{mn}}{2}\left[(\mathcal{U}^i_m + \mathcal{U}^j_m) - (\mathcal{U}^i_n + \mathcal{U}^j_n)\right]^2 \\ &- \sum_{m=1}^{N_\Gamma} \frac{\sigma_m}{2} \left[(\mathcal{U}^i_m - \mathcal{U}^j_m) - (\Psi^i_m - \Psi^j_m)\right]^2 - \frac{1}{2}\sum_{m=1}^{N}\sum_{n\in\mathcal{N}_m} \frac{\sigma_{mn}}{2}\left[(\mathcal{U}^i_m - \mathcal{U}^j_m) - (\mathcal{U}^i_n - \mathcal{U}^j_n)\right]^2 \Bigg\}, \end{aligned}$$

where $\mathcal{U}^i_m$ is the mth entry of the vector $\overline{\mathcal{U}}^i \in \mathbb{R}^N$.

3.2.2. Evaluation of entries $\Upsilon^{(2)}_{i,j}$

Consider two functions ψ_i, $\psi_j \in \Xi$, $i, j \in \{1, \dots, M-1\}$, and recall that Λ_0 is the DtN map of the reference medium with uniform conductivity $\sigma = 1$. We are going to compute $\langle \psi_i, \Lambda_0 \psi_j \rangle$ via $\langle \psi_i \pm \psi_j, \Lambda_0(\psi_i \pm \psi_j)\rangle$ using the polarization identity (36), where the quadratic form associated with Λ_0 is defined by

$$\langle \psi_i, \Lambda_0 \psi_i \rangle = \int_\Omega |\nabla u(\mathbf{x})|^2 \, d\mathbf{x}, \tag{28}$$

with the function $u \in H^1(\Omega)$ being a solution to

$$\begin{cases} -\nabla \cdot [\nabla u(\mathbf{x})] = 0, & \mathbf{x} \in \Omega, \\ u = \psi_i & \mathbf{x} \in \Gamma, \end{cases}$$

where $\psi_i \in \Xi$. The solution to this problem in the disk Ω could be found explicitly using the Poisson formula, that yields

$$\Upsilon^{(2)}_{i,j} = \begin{cases} k_i L^{2k_i}, & \text{if } i = j \\ 0, & \text{if } i \ne j \end{cases}$$

where k_i is the frequency mode of $\psi_i \in \Xi$ defined by (27), and L is the radius of the disk Ω.

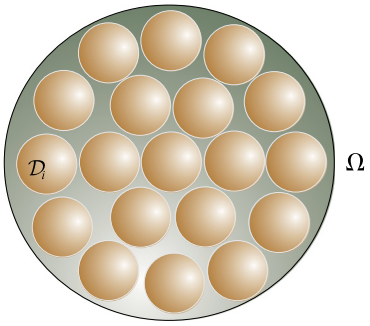

Fig. 2. The domain Ω with highly conducting inclusions $\mathcal{D}_i$, $i \in \{1, \dots, N\}$.

3.2.3. Evaluation of entries $\Upsilon^{(3)}_{i,j}$

Lastly, we find values $\Upsilon^{(3)}_{i,j}$. First, we consider the case of $i, j \le M/2$, that is, when $\psi_i = \frac{1}{\sqrt{\pi}} \cos i\theta$, $\psi_j = \frac{1}{\sqrt{\pi}} \cos j\theta$, and apply (26), (20) to obtain

$$\Upsilon^{(3)}_{i,j} = \frac{2}{\pi} \sum_{m=1}^{N_\Gamma} e^{-|i-j|\frac{\sqrt{2R\delta_m}}{L}} \mathcal{R}_{m,i\wedge j} \cos(i-j)\theta_m, \tag{29}$$

for $i, j \le M/2$, where $\mathcal{R}_{m,k}$ is defined by (21). Formula (29) also defines entries $\Upsilon^{(3)}_{i+M/2,j+M/2}$, $i, j < M/2$, that is, when $\psi_i = \frac{1}{\sqrt{\pi}} \sin i\theta$, $\psi_j = \frac{1}{\sqrt{\pi}} \sin j\theta$. Finally, we treat cases of $\Upsilon^{(3)}_{i,j+M/2}$, $i \le M/2, j < M/2$, when $\psi_i = \frac{1}{\sqrt{\pi}} \cos i\theta$, $\psi_{j+M/2} = \frac{1}{\sqrt{\pi}} \sin j\theta$, and $\Upsilon^{(3)}_{i+M/2,j}$, $i < M/2, j \le M/2$, when $\psi_{i+M/2} = \frac{1}{\sqrt{\pi}} \sin i\theta$, $\psi_j = \frac{1}{\sqrt{\pi}} \cos j\theta$ to have

$$\Upsilon^{(3)}_{i,j+M/2} = \Upsilon^{(3)}_{i+M/2,j} = -\frac{2}{\pi} \sum_{m=1}^{N_\Gamma} e^{-|i-j|\frac{\sqrt{2R\delta_m}}{L}} \mathcal{R}_{m,i\wedge j} \sin(i-j)\theta_m,$$

using (20), (26) as well.

3.3. Modification of the Schur complement system (4)

With matrix $\mathbf{\Lambda}$ constructed via procedure discussed in previous sections, one obtains $\mathbf{\Lambda}\overline{u}_\Gamma$, which is an approximation for normal derivative on the interface Γ. Then denote by $\Pi\mathbf{\Lambda}\overline{u}_\Gamma$ an approximation for the weak normal derivative on Γ, where Π is the matrix corresponding to the integral over the interface. Hence,

$$\Pi\mathbf{\Lambda}\overline{u}_\Gamma = \overline{\lambda}^\star_{1\Gamma}, \tag{30}$$

where $\overline{\lambda}^\star_{1\Gamma}$ is an approximation of weak normal derivative on Γ. Note that the FEM approximation for the weak normal derivative $\overline{\lambda}_{1\Gamma}$ of (7) differs from the newly introduced one $\overline{\lambda}^\star_{1\Gamma}$ of (30). However, we expect them to be close, which drives our choice for an approximation for the matrix $\mathrm{S}^{(1)}$, namely by $\Pi\mathbf{\Lambda}$. So we modify the Schur complement system (4) to obtain the following linear system

$$(\Pi\mathbf{\Lambda} + \mathrm{S}^{(2)})\overline{u}_\Gamma = \overline{g}^{(2)}_\Gamma. \tag{31}$$

Similarly to the discussion of Section 2.2.3, it can be solved using the PCG with the preconditioner $\mathrm{S}^{(2)}$.

4. Numerical experiments

4.1. Setup

In this section we demonstrate the efficiency of our heterogeneous domain decomposition approach. Let the domain Ω be a unit disk of radius $L = 1$ with $N = 19$ inclusions inside. All inclusions are identical disks of radii $R = 0.198$, and they are evenly distributed inside Ω, see Fig. 2. The smallest distance between neighboring inclusions $\mathcal{D}_i$ and $\mathcal{D}_j$ is $\delta_{ij} = 0.004$, while the distance between inclusions and the boundary $\partial\Omega = \Gamma$ is $\delta_i = 0.002$.

Suppose that the disk Ω is embedded in a disk $\hat{\Omega}$ of radius $\hat{L} = 3$, see Fig. 3. Our domain decomposition method is applied to the problem (1) defined in this $\hat{\Omega}$ using the procedure described in Section 2.2.3. In particular, we solve (31) for the approximation $\overline{u}_\Gamma$ of the solution on the interface Γ.

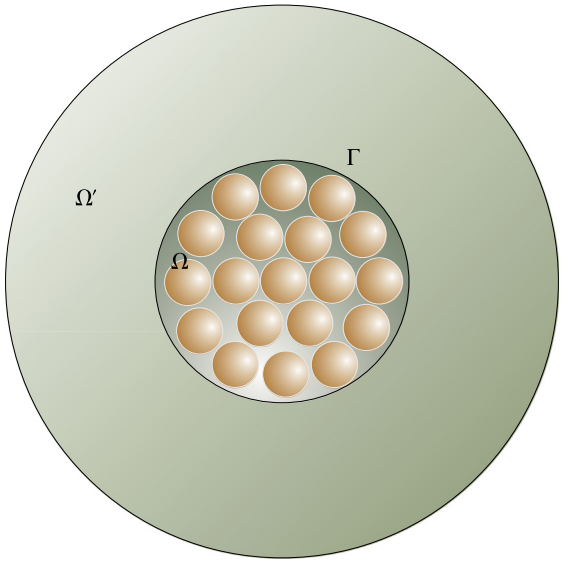

Fig. 3. The domain $\hat{\Omega}$ partitioned into subdomains Ω and Ω'.

We discretize the interface Γ with $M = 912$ points selected in a prescribed way. First, the closest points on Γ to the boundary neighboring inclusions are required to be in a discretization set of the points. Second, we select points equidistantly over Γ, that is, $\theta_i = \frac{2\pi}{M}(i-1)$, $i \in \{1, \dots, M\}$. Following the procedure described in Section 3.2 we obtain the matrix $\mathbf{\Lambda} \in \mathbb{R}^{M\times M}$, which is symmetric and positive semi-definite.

4.2. Numerical results

First, we examine the three asymptotic regimes of parameters R, δ and k that have been distinguished in [9]. In particular, the observations of [9] are follows. When the boundary potential ψ has low oscillations, the resistor network gets excited and $\mathcal{E}^{\text{net}}$ of (17) determines the leading order of the energy. If the boundary potential ψ is highly oscillatory ($k \gg 1$), the network plays no role, because it is not excited. In this case, the energy is approximately equal to that in the reference medium of conductivity 1, described by Λ_0 of (28). The 'resonant term' $\mathcal{R}[\psi]$ of (20)–(21) plays an important role in the approximation of energy when k gets intermediate values. Table 1 shows numerical illustration on how much influence each term has for the boundary potential ψ given by a single Fourier mode, that is, $\psi = \cos k\theta$.

Second, we perform our domain decomposition method for the setup described above. For this, the standard `pcg` function of MATLAB® with the preconditioner $\mathrm{S}^{(2)}$ is used to solve (31) with the initial guess $\overline{u}^0_\Gamma$ is zero vector, and the stopping criteria

$$\frac{\|(\Pi\mathbf{\Lambda} + \mathrm{S}^{(2)})\overline{u}^n_\Gamma - \overline{g}^{(2)}_\Gamma\|_2}{\|\overline{g}^{(2)}_\Gamma\|_2} \le \mathrm{tol} = 10^{-6},$$

and the relaxation parameter $\vartheta = 1/2$.

Because the analytical solution of (1) is not available, we compare the solution $\overline{u}^{\mathrm{DD}}_\Gamma$ obtained by the domain decomposition method described above to the solution $\overline{u}^{\mathrm{PL}}_\Gamma$, produced by the technique from [5], where PL stands for the *preconditioned Lancsoz*. We run experiments for different boundary potentials g, see Figs. 4–6. Table 2 displays the relative error between solutions of our domain decomposition (DD) and benchmarked preconditioned Lancsoz (PL) methods and the CPU times for both algorithms, that we discuss below.

From Table 2 we conclude that all solutions of our HDDM have demonstrated the relative error that is less than 7%, which is in agreement with the analysis of [9]. To the best of our knowledge, this is a very reasonable result for the hybrid method whose one essential component is of asymptotic nature. The discrepancies between our solution and the references one, which are clearly seen on the provided figures, correspond to the regions of the computational domain which were ignored in the asymptotic procedure construction, see [9] for the details. More specifically, a perfect match between the reference and proposed solutions is demonstrated, for example, at the points of the local maxima of both graphs for e.g. $\theta \in (-2, -1)$ in Fig. 4. These points of Γ lie within the computational domain where the asymptotic representation of Theorem 1 was done. However, the graph of the reference solution is slightly lower than one of the proposed HDD solution at two points of their local minima $\theta \in (-2, -1)$ in Fig. 4. These points lie in the domain that was completely ignored in the asymptotic procedure of [9] and is not taken into account in the asymptotic representation of Theorem 1. Similar discrepancies are observed at the

Table 2
Relative error between $\overline{u}_\Gamma^{\mathrm{DD}}$ and $\overline{u}_\Gamma^{\mathrm{PL}}$, and CPU time in seconds for the domain decomposition (DD) method of this paper and preconditioned Lancsoz (PL) method of [5].

g	$\frac{\|\overline{u}_\Gamma^{\mathrm{DD}}-\overline{u}_\Gamma^{\mathrm{PL}}\|_2}{\|\overline{u}_\Gamma^{\mathrm{PL}}\|_2}$	CPU (DD)	CPU (PL)
y^3	6.82%	0.96 s	3959.47 s
x	6.78%	0.99 s	3898.81 s
$3x+y^5$	6.86%	0.94 s	3847.92 s

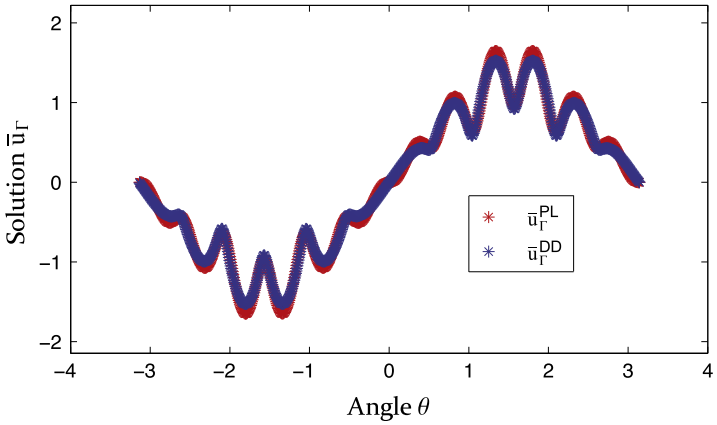

Fig. 4. Solutions $\overline{u}_\Gamma^{\mathrm{DD}}$ and $\overline{u}_\Gamma^{\mathrm{PL}}$ for $g=y^3$.

other points of local (max)minima of two graphs that cumulatively lead to a 7% error reported above, due to fact that these points lie in the domain which is disregarded by the asymptotic procedure of Theorem 1 used in our construction.

Although the both algorithms – the reference and the proposed ones – converge to a solution with the desired tolerance in a *couple of dozens iterations*, each iteration of our HDDM is significantly cheaper. To demonstrate this, we compare the CPU times of both numerical schemes performed on the same server, where the reported time corresponds to an iterative procedure itself, and does not include preprocessing steps. We remark that the main advantage of the method proposed above is that for a given geometry of the computational domain the evaluation of $\mathbf{\Lambda}$ is done offline, that is, once and for all boundary potentials.

We finally remark about the convergence of the employed method. Recall that in our construction we have utilized the Dirichlet–Neumann algorithm whose comprehensive convergence analysis can be found in [10]. In particular, the chosen iterative method is *optimal* as its rate of convergence is independent of the discretization size h.

Once solutions on the interface are found one can retrieve internal components of the solution. Solution $\overline{u}_2^{\mathrm{DD}}$ is defined by (6). Solution inside domain Ω and outside of a *boundary layer* (see [9] for the rigorous definition of the boundary layer) can be found as a linear interpolation of constant potentials on the inclusions $\mathcal{U}^i$ for $i\in\{1,\dots,N\}$. Inside the boundary layer within Ω, one can adopt an approximation of the solution given by formulas (4.54), (4.56), (4.57) in [9]. Since $\overline{u}_\Gamma^{\mathrm{DD}}$ and $\overline{u}_\Gamma^{\mathrm{PL}}$ are close and the matrix of system (2) is positive definite, internal solutions $\overline{u}_l^{\mathrm{DD}}$ and $\overline{u}_l^{\mathrm{PL}}$, $l\in\{1,2\}$, in the corresponding subdomains Ω and Ω' are close.

However, when the typical distance δ between particles is small compared their sizes as in our case, it is unpractical to evaluate u_1 by direct application of the formula (6) for any number N of particles, due to extremely fine meshes in the tiny gaps between particles, hence, computationally expensive inversion of the matrix $\mathrm{S}^{(1)}$. For the similar reasons, the approach developed in this paper can be useful in the construction of the multiscale methods, in which the precise solution inside the fine grid cell is not sought but rather an averaged response on the boundary.

5. Conclusions

This paper focuses on a construction of the efficient numerical scheme that can be used to solve high contrast PDEs (1) with rapidly oscillating coefficients. In particular, a high contrast composite medium that consists of the homogeneous part and a cluster of highly conducting particles close to one another was considered. A HDDM method that combines asymptotics by [9] in one subdomain with a FEM approximation in the other subdomain was proposed. The choice for the HDDM methodology was motivated by the fact that a FEM discretization in the high contrast subdomain is not feasible or computationally expensive.

We work with a two-dimensional domain since we were applying the results that were readily available by [9] developed for two dimensions. As an extension of asymptotics of [9] is possible for three dimensions, so is for our HDDM. All other

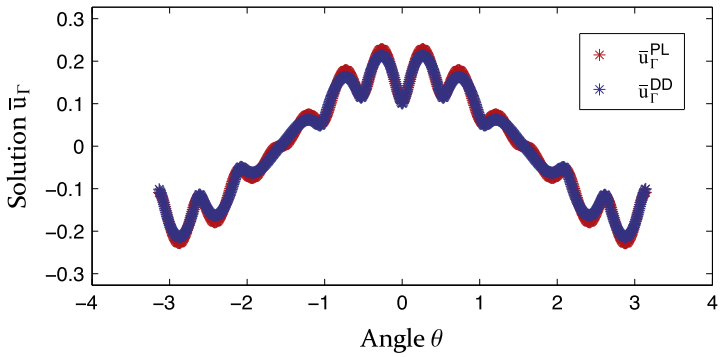

Fig. 5. Solutions $\bar{u}_\Gamma^{DD}$ and $\bar{u}_\Gamma^{PL}$ for $g = x$.

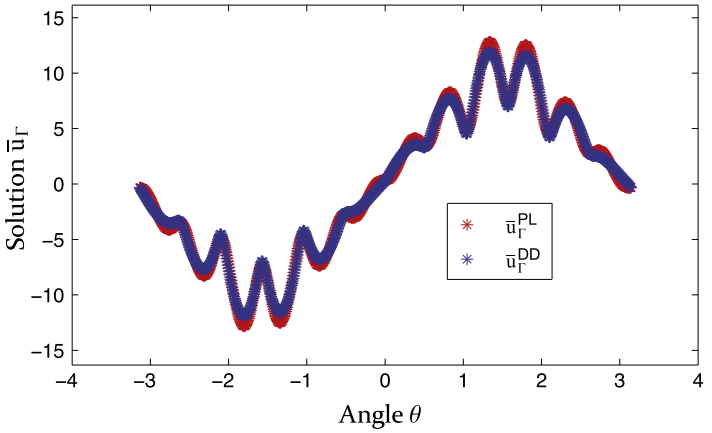

Fig. 6. Solutions $\bar{u}_\Gamma^{DD}$ and $\bar{u}_\Gamma^{PL}$ for $g = 3x + y^5$.

assumptions such as shapes of the domain Ω and particles $\mathcal{D}_i$ also inessential as the asymptotic formulas of [9] were dependent on curvatures of the boundaries at the points of the closest contact.

Numerical experiments of Section 4 demonstrate good qualitative results that provides hope that the proposed methodology might be applicable in designing multiscale strategies where the fine-scale features of the problem parameters cannot be resolved by the coarse solvers.

Acknowledgments

The authors were supported by the National Science Foundation grant DMS-1350248.

Appendix

A.1. Dirichlet-to-Neumann map Λ^{DtN}

In this paper, we consider the electrostatics PDE

$$-\nabla \cdot [\sigma(\mathbf{x})\nabla u(\mathbf{x})] = 0, \quad \mathbf{x} \in \Omega, \tag{32}$$

with a high contrast and rapidly varying nonnegative coefficient $\sigma(\mathbf{x})$ in a bounded, simply connected domain $\Omega \subset \mathbb{R}^d, d \geq 2$, that has smooth boundary. 'Rapidly varying' means that σ fluctuates on a length scale that is much smaller than the diameter of Ω, and 'high contrast' means that the ratio of the largest and smallest value of σ in Ω is very large, even infinite. Eq. (32) relates the voltage u and the associated electric field ∇u to the resulting current $\sigma(\mathbf{x})\nabla u$, where electrical conductivity $\sigma(\mathbf{x})$ is a positive symmetric matrix-valued function in Ω. This equation also determines a DtN map Λ^{DtN} that takes an arbitrary boundary voltage u on the boundary $\Gamma = \partial\Omega$ to the associated current flux on Γ:

$$\Lambda^{\mathrm{DtN}} : u(\mathbf{x}) \to \sigma(\mathbf{x})\nabla u(\mathbf{x}) \cdot \mathbf{n}(\mathbf{x}), \quad \mathbf{x} \in \Gamma, \tag{33}$$

where $\mathbf{n}(\mathbf{x})$ is the outward unit normal to Γ. The DtN map Λ^{DtN} is ultimately connected with the spectral properties of the corresponding differential operator in (32), and has attracted a lot of attention in the last decade, see e.g. [14] and references therein. Consider the solution $u \in H^1(\Omega)$ of (32) satisfying the Dirichlet data:

$$u(\mathbf{x}) = \psi(\mathbf{x}), \quad \mathbf{x} \in \Gamma, \quad \text{where } \psi \in H^{1/2}(\Gamma) \text{ is some given function.} \tag{34}$$

Recall that if ψ is constant then the solution u of (32), (34) is also constant, so it is natural to restrict attention to the subspace

$$H^{1/2}_{\dagger}(\Gamma) = H^{1/2}(\Gamma) \cap \left\{ u \in L^2(\Gamma) : \int_{\Gamma} u \, ds = 0 \right\}. \tag{35}$$

Then the solution $u \in H^1(\Omega)$ of (32), (34) with $\psi \in H^{1/2}_{\dagger}(\Gamma)$ also solves the variational problem

$$\mathcal{E}_{\psi} := \min_{u|_{\Gamma}=\psi} \int_{\Omega} \sigma(\mathbf{x}) \nabla u(\mathbf{x}) \cdot \nabla u(\mathbf{x}) \, d\mathbf{x},$$

and the minimal energy $\mathcal{E}_{\psi}$ is determined by Λ^{DtN} since

$$\int_{\Omega} \sigma(\mathbf{x}) \nabla u \cdot \nabla u \, d\mathbf{x} = \int_{\Gamma} \psi \ \Lambda^{\mathrm{DtN}} \psi \ ds =: \langle \psi, \Lambda^{\mathrm{DtN}} \psi \rangle.$$

The converse is also true, namely, the minimum energy $\mathcal{E}_{\psi}$ for all Dirichlet data ψ determines the boundary map Λ^{DtN} through *the polarization identity*:

$$\text{For all } \psi, \ \varphi \in H^{1/2}_{\dagger}(\Gamma): \ 4 \int_{\Gamma} \psi \ \Lambda^{\mathrm{DtN}} \varphi \, ds = \langle (\psi + \varphi), \Lambda^{\mathrm{DtN}}(\psi + \varphi) \rangle - \langle (\psi - \varphi), \Lambda^{\mathrm{DtN}}(\psi - \varphi) \rangle. \tag{36}$$

With all the above, the map $\Lambda^{\mathrm{DtN}} : H^{1/2}_{\dagger}(\Gamma) \to H^{-1/2}_{\dagger}(\Gamma)$ with $H^{-1/2}_{\dagger}(\Gamma) = H^{-1/2}(\Gamma) \cap \left\{ \int_{\Gamma} u \, ds = 0 \right\}$, is positive and symmetric with respect to the L^2-inner product, and invertible. Hence, it defines a positive-definite quadratic form

$$\langle \psi, \Lambda^{\mathrm{DtN}} \varphi \rangle = \int_{\Gamma} \psi \ \Lambda^{\mathrm{DtN}} \varphi \, ds = \int_{\Omega} \sigma(\mathbf{x}) \nabla u(\mathbf{x}) \cdot \nabla v(\mathbf{x}) \, d\mathbf{x}$$

on $H^{1/2}_{\dagger}(\Gamma)$, where u, v solve (32) with Dirichlet boundary conditions ψ, φ on Γ, respectively.

The simplest special case of (32), when $\sigma(\mathbf{x}) \equiv 1$ with the solution $u \in H^1(\Omega)$ being *harmonic*, is extensively studied. Another well-understood case where a lot is known about the energy that defines the associated DtN map, is when $\sigma(\mathbf{x})$ is uniform except for a constant conductivity $\sigma(\mathbf{x}) = \sigma_o$ in some part of the domain $\mathcal{D} \subset \Omega$. The least studied and challenging case is when $\sigma_o \to \infty$ on $\mathcal{D}$ that describes the so-called *high contrast problem* (see [15] for the relation between the DtN map of high contrast problem and the limiting case of $\sigma_o = \infty$ sometimes referred to as an *infinite contrast* case). In this paper, we study this latter case, whose mathematical formulation is given in (1), that is, we seek for an approximation of the DtN map of two phase composites with perfectly conducting ($\sigma = \infty$) inclusions in a medium of the unit conductivity ($\sigma = 1$). The relation between solutions of *high but finite contrast* case and *infinite contrast* one has been investigated in [16].

A.2. Auxiliary facts

In this section, we will prove some auxiliary facts used above.

Lemma 1. *Consider the local conductances σ_{ij}, $i \in \{1, \dots, N\}$, $j \in \mathcal{N}_i$, and σ_i, $i \in \{1, \dots, N_\Gamma\}$ given by (19) and the vector of boundary potential $\overline{\Psi}[\psi] \in \mathbb{R}^{N_\Gamma}$ by (18). Then a vector $\overline{\mathcal{U}} \in \mathbb{R}^N$ is the minimizer of (17) if and only if $\overline{\mathcal{U}}$ is the solution of equation $\mathcal{M}\overline{\mathcal{U}} = \overline{\mathcal{P}}$, where the entries of the matrix $\mathcal{M} \in \mathbb{R}^{N \times N}$ are defined by*

$$\mathcal{M}_{ij} = \begin{cases} \sigma_i + \sum\limits_{l \in \mathcal{N}_i} \sigma_{il}, & \text{if } i \in \{1, \dots, N_\Gamma\}, \ i = j \\ \sum\limits_{l \in \mathcal{N}_i} \sigma_{il}, & \text{if } i \in \{N_\Gamma + 1, \dots, N\}, \ i = j \\ -\sigma_{ij}, & \text{if } i \in \{1, \dots, N\}, \ j \in \mathcal{N}_i \\ 0, & \text{if } i \in \{1, \dots, N\}, \ j \notin \mathcal{N}_i \end{cases} \tag{37}$$

and entries of the vector $\overline{\mathcal{P}} \in \mathbb{R}^N$ are by

$$\mathcal{P}_i = \begin{cases} \sigma_i \Psi_i, & \text{if } i \in \{1, \dots, N_\Gamma\}, \\ 0, & \text{if } i \in \{N_\Gamma + 1, \dots, N\}. \end{cases} \tag{38}$$

Proof ($\Rightarrow$). To minimize (17) we compute the partial derivatives of $\mathcal{E}^{\text{net}}$ for all $i \in \{1, \dots, N\}$ and set them equal to zero:

$$0 = \frac{\partial \mathcal{E}^{\text{net}}}{\partial \mathcal{U}_i} = \begin{cases} \sigma_i(\mathcal{U}_i - \Psi_i) + \sum\limits_{j\in\mathcal{N}_i} \sigma_{ij}(\mathcal{U}_i - \mathcal{U}_j), & \text{if } i \in \{1, \dots, N_\Gamma\}, \\ \sum\limits_{j\in\mathcal{N}_i} \sigma_{ij}(\mathcal{U}_i - \mathcal{U}_j), & \text{if } i \in \{N_\Gamma + 1, \dots, N\}, \end{cases}$$

that gives rise to the following equations with respect to the entries $\mathcal{U}_i$ of the vector $\overline{\mathcal{U}}$:

$$\begin{cases} \left(\sigma_i + \sum\limits_{j\in\mathcal{N}_i} \sigma_{ij}\right)\mathcal{U}_i - \sum\limits_{j\in\mathcal{N}_i} \sigma_{ij}\mathcal{U}_j = \sigma_i\Psi_i, & \text{if } i \in \{1, \dots, N_\Gamma\}, \\ \sum\limits_{j\in\mathcal{N}_i} \sigma_{ij}\mathcal{U}_i - \sum\limits_{j\in\mathcal{N}_i} \sigma_{ij}\mathcal{U}_j = 0, & \text{if } i \in \{N_\Gamma + 1, \dots, N\}. \end{cases}$$

These equations yield (37) and (38).

($\Leftarrow$) To establish the sufficient condition, we have to prove that the matrix $\mathcal{R} = [\mathcal{R}_{ij}]$ of second derivatives $\mathcal{R}_{ij} = \frac{\partial^2 \mathcal{E}^{\text{net}}}{\partial \mathcal{U}_i \partial \mathcal{U}_j}$ whose entries are

$$\mathcal{R}_{ij} = \begin{cases} \sigma_i + \sum\limits_{m=1}^{N} \sigma_{im}, & \text{if } i = j, \\ -\sigma_{ij}, & \text{if } i \neq j \end{cases}$$

is positive-definite. All inclusions are assumed to be adjacent to the boundary and each other (if not, some σ_i and σ_{ij} would be zero that does not affect positive-definiteness of the matrix).

We show that this matrix is positive-definite by induction over the number of inclusions and proceed by induction. Then for the case of two inclusions, that is, for $\alpha \in \mathbb{R}$, we consider the quadratic form

$$\begin{aligned} &\begin{pmatrix} 1 & \alpha \end{pmatrix} \begin{pmatrix} \sigma_1 + \sigma_{11} + \sigma_{12} & -\sigma_{12} \\ -\sigma_{12} & \sigma_2 + \sigma_{12} + \sigma_{22} \end{pmatrix} \begin{pmatrix} 1 \\ \alpha \end{pmatrix} \\ &= \sigma_1 + \sigma_{11} + \sigma_{12} - 2\alpha\sigma_{12} + \alpha^2(\sigma_2 + \sigma_{12} + \sigma_{22}). \end{aligned}$$

The minimizer of this quadratic form is

$$\alpha_{\min} = \frac{\sigma_{12}}{\sigma_2 + \sigma_{12} + \sigma_{22}},$$

and the minimum of quadratic form is

$$\frac{\sigma_1\sigma_2 + \sigma_1\sigma_{12} + \sigma_1\sigma_{22} + \sigma_{11}\sigma_2 + \sigma_{11}\sigma_{12} + \sigma_{11}\sigma_{22} + \sigma_{12}\sigma_2 + \sigma_{12}\sigma_{22}}{\sigma_2 + \sigma_{12} + \sigma_{22}} > 0.$$

So quadratic form is positive-definite for any $\alpha \in \mathbb{R}$ in the case of two inclusions. Assume that matrix is positive definite for l inclusions, that is, for all $\overline{\alpha} \in \mathbb{R}^l$ or

$$\sum_{i=1}^{l}\sum_{j=1}^{l} \alpha_i \mathcal{R}_{ij} \alpha_j > 0. \tag{39}$$

Now we proceed by induction argument and consider the quadratic form corresponding to $l + 1$ inclusions:

$$\begin{pmatrix} \overline{\alpha}^T & 1 \end{pmatrix} \begin{pmatrix} \mathcal{R}^* & -\beta \\ -\beta^T & \sigma_{l+1} + \sum\limits_{i=1}^{l+1} \sigma_{i\,l+1} \end{pmatrix} \begin{pmatrix} \overline{\alpha} \\ 1 \end{pmatrix}, \tag{40}$$

where $\beta = (\sigma_{1\,l+1}, \dots, \sigma_{l\,l+1}) \in \mathbb{R}^l$ and

$$\mathcal{R}^*_{ij} = \begin{cases} \mathcal{R}_{ij}, & \text{if } i \neq j, \\ \mathcal{R}_{ij} + \sigma_{i\,l+1}, & \text{if } i = j. \end{cases}$$

Expanding (40), we have

$$\begin{aligned} &\sum_{j=1}^{l} \alpha_j \sum_{i=1}^{l} \alpha_i \mathcal{R}^*_{ij} - 2\sum_{i=1}^{l} \alpha_i\beta_i + \sigma_{l+1} + \sum_{i=1}^{l+1} \sigma_{i\,l+1} \\ &= \sum_{j=1}^{l} \alpha_j \left(\sum_{i=1}^{l} \alpha_i \mathcal{R}_{ij} + \alpha_j\sigma_{j\,l+1}\right) - 2\sum_{i=1}^{l} \alpha_i\sigma_{i\,l+1} + \sigma_{l+1} + \sum_{i=1}^{l+1} \sigma_{i\,l+1} \end{aligned}$$

$$= \sum_{j=1}^{l} \alpha_j \sum_{i=1}^{l} \alpha_i \mathcal{R}_{ij} + \sum_{i=1}^{l} \alpha_i^2 \sigma_{i\,l+1} - 2 \sum_{i=1}^{l} \alpha_i \sigma_{i\,l+1} + \sigma_{l+1} + \sigma_{l+1\,l+1} + \sum_{i=1}^{l} \sigma_{i\,l+1}$$

$$= \sum_{j=1}^{l} \alpha_j \sum_{i=1}^{l} \alpha_i \mathcal{R}_{ij} + \sigma_{l+1}\sigma_{l+1\,l+1} + \sum_{i=1}^{l} \sigma_{i\,l+1}(\alpha_i^2 - 2\alpha_i + 1).$$

Since $\alpha_i^2 - 2\alpha_i + 1 \geq 0$ and by the inductive step (39), we obtain that the quadratic form (40) is positive for all $\overline{\alpha} \in \mathbb{R}^l$. Thus, matrix $\mathcal{R}$ is positive definite for any number of inclusions and $\overline{\mathcal{U}}$ is indeed the minimizer of (17). □

Lemma 2. *If the boundary potential $\overline{\Psi}$ in (17) is a sum of two terms $\overline{\Psi} = \overline{\Psi}^{(1)} + \overline{\Psi}^{(2)}$ then the minimizer of (17) is a sum of two terms $\overline{\mathcal{U}} = \overline{\mathcal{U}}^{(1)} + \overline{\mathcal{U}}^{(2)}$, where $\overline{\mathcal{U}}^{(i)}$ is a minimizer of (17) with boundary potential $\overline{\Psi}^{(i)}$, $i \in \{1, 2\}$.*

Proof. By Lemma 1 minimizers of (17) with boundary potentials $\overline{\Psi}^{(1)}$ and $\overline{\Psi}^{(2)}$ satisfy $\mathcal{M}\overline{\mathcal{U}}^{(1)} = \overline{\mathcal{P}}^{(1)}$ and $\mathcal{M}\overline{\mathcal{U}}^{(2)} = \overline{\mathcal{P}}^{(2)}$, respectively. So $\mathcal{M}\overline{\mathcal{U}}^{(1)} + \mathcal{M}\overline{\mathcal{U}}^{(2)} = \overline{\mathcal{P}}^{(1)} + \overline{\mathcal{P}}^{(2)}$. Hence, by the same lemma, $\overline{\mathcal{U}}^{(1)} + \overline{\mathcal{U}}^{(2)}$ is a minimizer of (17) corresponding to the boundary potential $\overline{\Psi}^{(1)} + \overline{\Psi}^{(2)}$. □

References

[1] J. Galvis, E. Chung, Y. Efendiev, W.T. Leung, On overlapping domain decomposition methods for high-contrast multiscale problems, 2017. preprint: arXiv:1705.09004.
[2] J. Mandel, Marian Brezina, Balancing domain decomposition for problems with large jumps in coefficients, Math. Comp. 65 (216) (1996) 1387–1401.
[3] J. Galvis, Y. Efendiev, Yalchin, Domain decomposition preconditioners for multiscale flows in high-contrast media, Multiscale Model. Simul. 8 (4) (2010) 1461–1483.
[4] B. Aksoylu, H. Klie, A family of physics-based preconditioners for solving elliptic equations on highly heterogeneous media, Appl. Numer. Math. IMACS J. 59 (6) (2009) 1159–1186.
[5] Y. Gorb, D. Kurzanova, Y. Kuznetsov, A Robust Preconditioner for High-Contrast Problems, 2018. preprint: arXiv:1801.01578.
[6] A. Quarteroni, F. Pasquarelli, A. Valli, Heterogeneous domain decomposition principles, algorithms, applications, in: D.E. Keyes, T.F. Chan, G.A. Meurant, J.S. Scroggs, R.G. Voigt (Eds.), Fifth International Symposium on Domain Decomposition Methods for Partial Differential Equations, SIAM, Philadelphia, PA, 1992, pp. 129–150.
[7] A. Quarteroni, A. Valli, Domain decomposition methods for partial differential equations, in: Numerical Mathematics and Scientific Computation, Oxford University Press, New York, 1999.
[8] Y. Efendiev, T.Y. Hou, Multiscale finite element methods, in: Surveys and Tutorials in the Applied Mathematical Sciences: Theory and Applications, Vol. 4, Springer, New York, 2009.
[9] L. Borcea, Y. Gorb, Y. Wang, Asympthotic approximation of the Dirichlet-to-Neumann map of high contrast conductive media, SIAM Multiscale Model. Simul. 12 (4) (2014) 1494–1532.
[10] A. Toselli, O. Widlund, Domain Decomposition Methods–Algorithms and Theory, in: Springer Series in Computational Mathematics, vol. 34, Springer-Verlag, Berlin, 2005.
[11] P.E. Bjørstad, O.B. Widlund, Iterative methods for the solution of elliptic problems on regions partitioned into substructures, SIAM J. Numer. Anal. 23 (6) (1986) 1097–1120.
[12] F. Aurenhammer, R. Klein, D.-T. Lee, Voronoi Diagrams and Delaunay Triangulations, World Scientific Publishing Co. Pte. Ltd., Hackensack, NJ, 2013.
[13] L. Lewin, Polylogarithms and Associated Functions, North-Holland, Amsterdam, 1981.
[14] J. Behrndt, A.F.M. ter Elst, Dirichlet-to-Neumann maps on bounded Lipschitz domains, J. Differential Equations 259 (11) (2015) 5903–5926.
[15] R.V. Kohn, H. Shen, M.S. Vogelius, M.I. Weinstein, Cloaking via change of variables in electric impedance tomography, Inverse Problems 24 (1) (2008) 015016(21).
[16] V.M. Calo, Y. Efendiev, J. Galvis, Asymptotic expansions for high-contrast elliptic equations, Math. Models Methods Appl. Sci. 24 (3) (2014) 465–494.